Functionalization of Chlorotonils: Dehalogenil as Promising Lead Compound for In Vivo Application

Walter Hofer, Felix Deschner, Gwenaëlle Jézéquel, Laìs Pessanha de Carvalho, Noran Abdel-wadood, Linda M Pätzold, Steffen Bernecker, Bernd Morgenstern, Andreas M Kany, Miriam M Große, et al.

How to cite: *Angew. Chem. Int. Ed.* **2024**, *63*, e202319765
doi.org/10.1002/anie.202319765

Natural Products

Functionalization of Chlorotonils: Dehalogenil as Promising Lead Compound for In Vivo Application

Walter Hofer, Felix Deschner, Gwenaëlle Jézéquel, Laìs Pessanha de Carvalho, Noran Abdel-Wadood, Linda Pätzold, Steffen Bernecker, Bernd Morgenstern, Andreas M. Kany, Miriam Große, Marc Stadler, Markus Bischoff, Anna K. H. Hirsch, Jana Held, Jennifer Herrmann, and Rolf Müller**

Abstract: The natural product chlorotonil displays high potency against multidrug-resistant Gram-positive bacteria and *Plasmodium falciparum.* Yet, its scaffold is characterized by low solubility and oral bioavailability, but progress was recently made to enhance these properties. Applying late-stage functionalization, we aimed to further optimize the molecule. Previously unknown reactions including a sulfur-mediated dehalogenation were revealed. **Dehalogenil**, the product of this reaction, was identified as the most promising compound so far, as this new derivative displayed improved solubility and in vivo efficacy while retaining excellent antimicrobial activity. We confirmed superb activity against multidrug-resistant clinical isolates of *Staphylococcus aureus* and *Enterococcus* spp. and mature transmission stages of *Plasmodium falciparum.* We also demonstrated favorable in vivo toxicity, pharmacokinetics and efficacy in infection models with *S. aureus.* Taken together, these results identify **dehalogenil** as an advanced lead molecule.

Introduction

Natural products represent an important pool of chemical diversity to cover the need of new scaffolds in drug discovery.[1,2] These scaffolds have the major advantage of displaying wider structural diversity than most synthetically obtained libraries including clinically approved drugs.[3] This diversity is often derived from evolutionary optimization for biological activity, and in most cases cannot be easily accessed by classic organic synthesis. Total synthesis is one elegant way to functionalize those scaffolds, though their length, complexity, and their insufficient yields often stop efforts to access natural products on large scale. However, semisynthetic approaches are used to derivatize potent natural products towards novel drug candidates.[4–7] In particular, antimicrobial compounds traditionally relied on such strategies, since they could be isolated in high yields from microbial fermentation and later used as starting material for semisyntheses.

In recent years, antimicrobial resistance increased at an alarming rate. Especially multidrug-resistant bacteria over-

[*] Dr. W. Hofer, F. Deschner, Dr. G. Jézéquel, Dr. A. M. Kany, Prof. A. K. H. Hirsch, Dr. J. Herrmann, Prof. R. Müller
Helmholtz Institute for Pharmaceutical Research Saarland (HIPS)
Helmholtz Centre for Infection Research (HZI) and Department of Pharmacy at Saarland University
Campus Building E8.1, 66123 Saarbrücken, Germany
E-mail: Jennifer.herrmann@helmholtz-hips.de
rolf.mueller@helmholtz-hips.de

Dr. W. Hofer, F. Deschner, Dr. G. Jézéquel, L. Pessanha de Carvalho, Dr. A. M. Kany, Dr. M. Große, Prof. M. Stadler, Prof. A. K. H. Hirsch, Dr. J. Held, Dr. J. Herrmann, Prof. R. Müller
German Centre for Infection Research (DZIF)
Braunschweig, 38124 Germany

L. Pessanha de Carvalho, Dr. J. Held
Institute of Tropical Medicine
Eberhard Karls University Tübingen
Wilhelmstraße 27, 72074 Tübingen, Germany

N. Abdel-Wadood, L. Pätzold, Prof. M. Bischoff
Institute for Medical Microbiology and Hygiene
Saarland University
66421 Homburg, Germany

N. Abdel-Wadood
Institute of Anatomy and Cell Biology /
Saarland University
66421 Homburg, Germany

S. Bernecker, Dr. M. Große, Prof. M. Stadler
Microbial Drugs
Helmholtz Centre for Infection Research (HZI)
Inhoffenstraße 7, 38124 Braunschweig, Germany

Dr. B. Morgenstern
Inorganic Solid State Chemistry
Saarland University
Campus, 66123 Saarbrücken, Germany

Dr. J. Held
Centre de Recherches Médicales de Lambaréné
Lambaréné, BP 242BP 242 Gabon

Prof. A. K. H. Hirsch, Prof. R. Müller
Helmholtz International Lab for Anti-Infectives
Saarbrücken, 66123 Germany

coming last resort antibiotics pose a severe threat to public health.[8–11] Other pathogens such as the malaria parasites *Plasmodium falciparum* and *Plasmodium vivax* are also showing increased resistance against the standard medications,[12,13] and effective and safe alternatives against the transmission stages are highly wanted.[14] Thus, the need for new, resistance-breaking antimicrobial and antiparasitic compounds with novel targets is high, especially in view of the fact that only six new antibiotic classes were introduced during the last five decades.[15–18]

Chlorotonils are a new substance class showing strong antimicrobial and antiplasmodial activities. Chlorotonil A (**1**) is the main product of fermentation from *Sorangium cellulosum* So ce1525 and comprises a 14-membered cyclic lactone featuring a unique *gem*-1,3-dichlorodione moiety (Figure 1).[19] Fermentation further yields mono-chlorinated derivatives chlorotonil B1 (**2**) and B2 (**3**). A 14-membered macrolide core structure is also present in clinically used antibiotics (e.g. erythromycin, clarithromycin),[20–22] yet chlorotonils show significant differences in their structure and biological activity and therefore clearly represent a new class of anti-infectives. Although **1** and **2** displayed promising antimicrobial activities,[23–25] the major disadvantage of this molecular scaffold is its low solubility. We recently reported the transformation of **1** into **2**, together with a stereoselective epoxidation, and epoxide ring opening improving physicochemical properties of the class,[25] resulting in the first generation frontrunner ChB1-Epo2 **4** (Figure 1). We were able to determine blood concentrations after oral administration and we demonstrated in vivo efficacy in an *S. aureus* thigh infection model.[25] Unfortunately, the epoxidation led to reduced activity against *Plasmodium* spp. together with some increase in toxicity as reported in this work. In addition, more detailed structure–activity relationship (SAR) studies are lacking, and aspects such as in vivo availability, solubility and safety still require improvement to further increase in vivo efficacy. Therefore, two different approaches (isolation of fermentation side products and semisynthesis) were performed herein to obtain new derivatives. These efforts led to the identification of a second-generation frontrunner, which was nominated as lead molecule after extensive profiling.

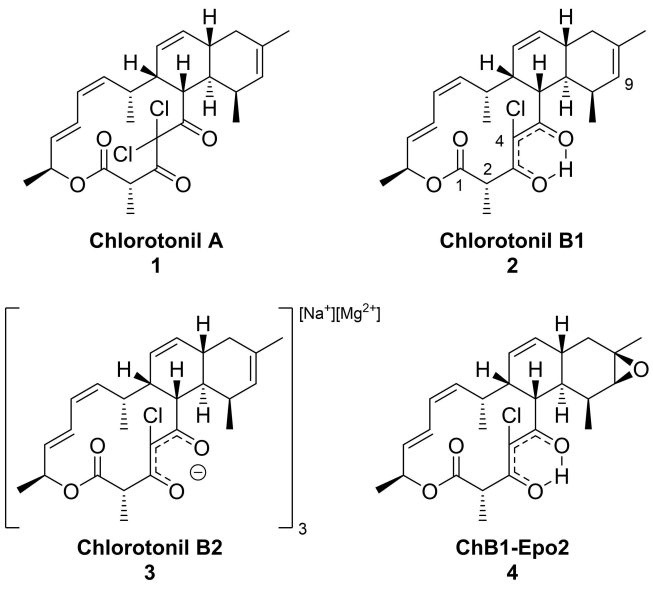

Figure 1. Structures of chlorotonil A **1**, chlorotonil B1 **2**, chlorotonil B2 **3**, and semisynthetic epoxide ChB1-Epo2 **4**.[19,25]

Results and Discussion

The starting point of the derivatization was the fermentation of So ce1525 described before.[19,25] Larger amounts of crude extracts containing chlorotonils were obtained and minute amounts of minor products (SI Figure 1, substances **SI1-5**) were analyzed. Here, we could identify multiple variations of chlorotonils, including a dimer and C2-demethylation products.

In the next step, we conducted a wide series of reactions on different chlorotonils in order to modify the different functionalities/positions in the molecule with the aim to learn as much as possible about the SAR of this molecule class. The starting materials were obtained either directly from the fermentation, or from a one-step dechlorination of **1** as described in Scheme 1. We found conditions for transformation of almost pure mixtures of **1/3** to pure **2** with 80 % to quantitative yields (Scheme 1) and, thus, no need for further purification prior to subsequent semisynthetic reactions.

Ultimately, we managed to obtain **1** and **2** on gram-scale providing a good starting point for semisyntheses. We used this material to screen numerous reactions conditions, and found that chlorotonils were inert under most conditions or decomposed (SI Tables 1A–H). As a side note, we noticed a lack of reactivity of chlorotonils with even strong reagents such as $KMnO_4$ or diethylaminosulfur trifluoride during our work. Nevertheless, several transformations highlighted new reactivity and led to promising compounds.

Previously, we showed that **1** can easily lose one of the geminal chlorines at C4 and identified this transformation as potential in vivo safety concern.[25] We decided to substitute one or both chlorines by the Finkelstein (type) reaction to see whether there would be an effect on activity.[26] Direct substitution to fluoride, bromide and iodide was not possible in acetone, *N*,*N*-dimethylformamide (DMF) or acetonitrile with either **1**, **2** or **3**. Instead, we obtained an unexpected bridged derivative, which we further substituted (SI

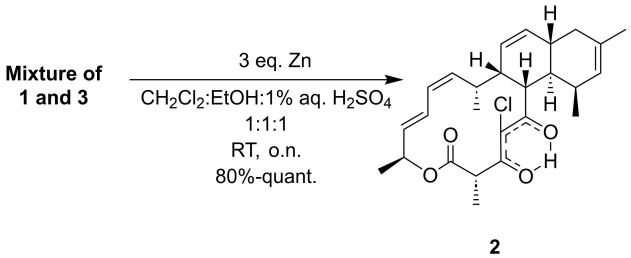

Scheme 1. Optimized transformation of **1/3** to **2**. Aq.: aqueous.

Scheme 1, compounds **SI6-8**). The possible reaction mechanism is depicted in Supporting Information Scheme 2.

Inspired by the total synthesis of **1**,[28] we investigated the electrophilic substitution at C4 starting from **2** as we wanted to explore the influence of C3-5 modifications on SAR. Here, we obtained **1** using *N*-chlorosuccinimide (NCS) and pyridine in 71 % yield (Scheme 2).

When **1** was treated under the same conditions in the presence of *p*-toluene sulfonic acid (*p*TSA), chlorination at C9 occurred (**SI9**, possible mechanism in Supporting Information Scheme 3 and conditions screening in Supporting Information Table 2). Fluorination with *N*-fluorobenzenesulfoneimide (NFSI) led to fluorine introduction (**5**, Scheme 2). Treatment with *N*-bromo or *N*-iodo succinimide in the presence of a base led to the corresponding halide insertion or exchange of chloride and was confirmed by mass spectrometry. Nevertheless, isolation was impossible due to decomposition on the solid phase under normal and reversed phase conditions.

Still in the aim of exploring SAR at this position, a C4-regio- and stereoselective methylated product was obtained with either NaH or potassium *tert*-butoxide (**6**, Scheme 2) and verified by X-ray diffraction. Interestingly, C2-methylation occurred when employing lithium bis(trimethylsilyl)amide (LiHMDS), leading to **7**, which complemented C2 SAR together with the natural products **SI1** and **SI2**. In an attempt to introduce a thiol group at C4 in **2** using elemental sulfur and KOtBu (potassium tert-butoxide), we unexpectedly observed dehalogenation rather than thiol insertion resulting in **dehalogenil** (**8**) with medium yield (Scheme 2). Interested in this new product, we also managed to obtain **8** by photochemical elimination, and as a 1:1 epimeric mixture after methylation of natural **SI2** with LiHMDS, however, in low yields. We then strived for condition optimization of the sulfur-mediated dehalogenation from **2** (SI Table 3) due to its initial superb activity and improved solubility.

During the optimization, several new side products were isolated from the pooled mixture (SI Figure 2, compounds **9–13**). The formation of these byproducts led to a proposed mechanism via a thiozonide (deep blue reaction mixture) attack at C4 with a subsequent elimination (Scheme 3). In the past, the thiozonide was reported to eliminate allylic bromides or was used for the formation of heterocycles.[29–33]

Dehalogenil is especially remarkable because it was impossible to obtain it from fermentation of So ce1525 due to the specificity of C2 methylation in the biosynthesis requiring two Cl atoms.[19] Additionally, **dehalogenil** was not found to form complexes with metal carbonates in toluene/methanol as reported before for **2** and was therefore ruled out as a direct complexing reagent under these conditions.[25]

In addition, as the epoxidation of **2** previously gave interesting results especially in terms of solubility,[25] we synthesized the two diastereoisomers **14** and **15** in a regioselective fashion using *meta*-chloroperoxybenzoic acid (*m*CPBA) in CH_2Cl_2 (Scheme 4).

Finally, we also explored macrocycle opening and rearrangement reactions yielding several other molecules of interest for SAR studies (SI Schemes 4–8, compounds **SI10-17**).[34–36]

Our combined approaches led to 27 new derivatives of the chlorotonil class (five natural products and 22 semi-synthetic compounds), which were all subjected to bioactivity testing against a panel of bacteria as well as *P. falciparum* (Table 1).

Activities between the chloroquine-sensitive (3D7) and the chloroquine-resistant (D2d) *P. falciparum* strains were nearly identical for most compounds, confirming the superb

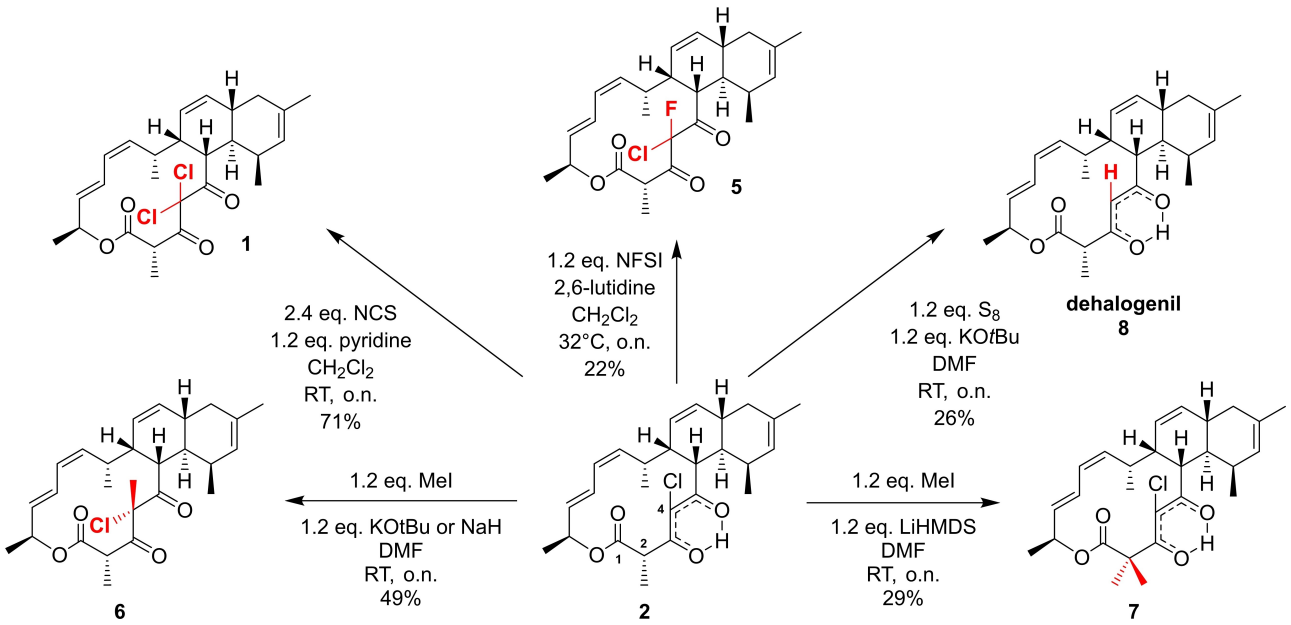

Scheme 2. Transformation of **2** into chlorinated, fluorinated, methylated, and dehalogenated derivatives. KOtBu: potassium *tert*-butoxide; NCS: *N*-chlorosuccinimide; NFSI: *N*-fluorobenzenesulfoneimide; LiHMDS: lithium bis(trimethylsilyl)amide.

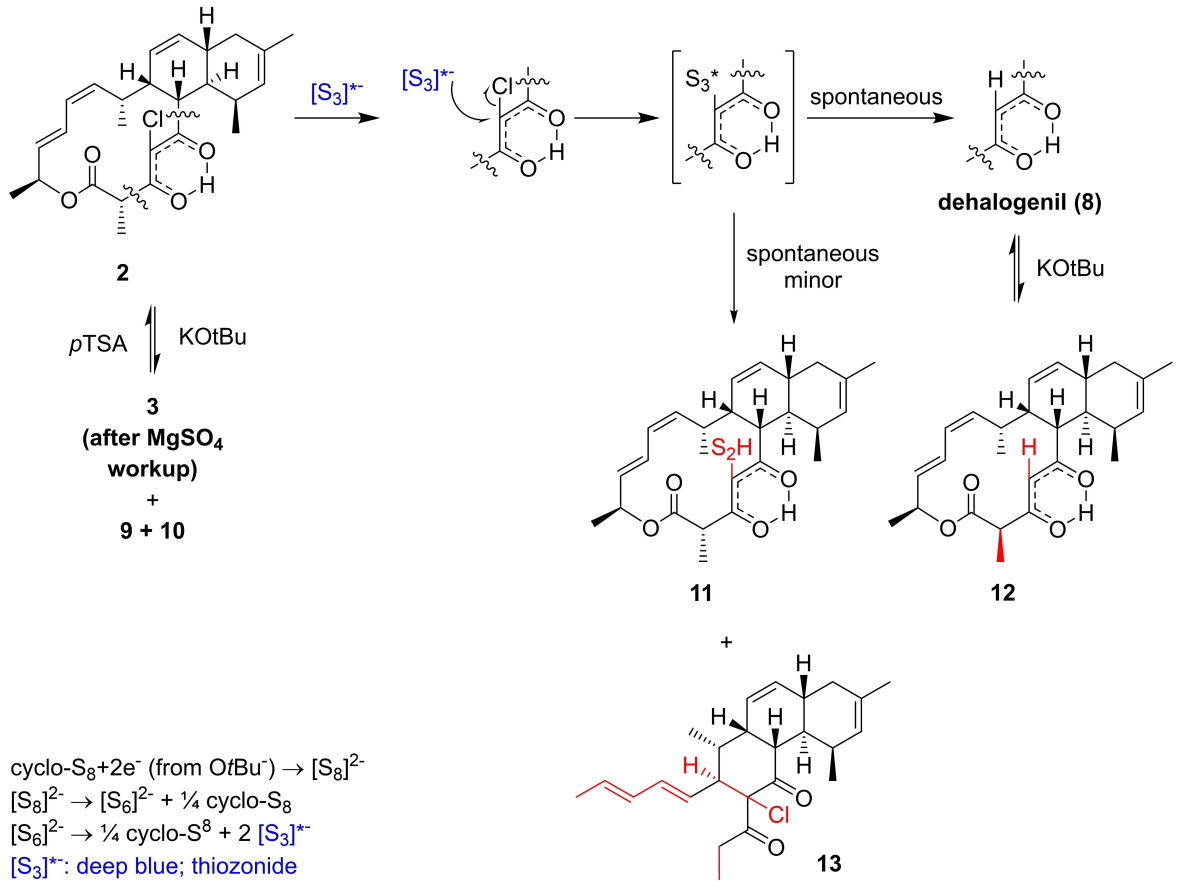

Scheme 3. Proposed dehalogenation of **2** based on the observed side products. First, elemental sulfur reacts with KOtBu to the observed deep blue thiozonide, which replaces chlorine forming an instable intermediate. The intermediate then either spontaneously eliminates sulfur to form **dehalogenil** or thiotonil (**11**). In the presence of KOtBu, **2** can either form salts (**9**, **3** after workup), which is reversible with *p*TSA acting as acid. Additionally, epimerization of **2** or **8** can occur (**10** or **12**, respectively). It was also possible to isolate a chlorinated rearrangement product (**13**) from the dehalogenation optimization. *p*TSA: *p*-toluene sulfonic acid

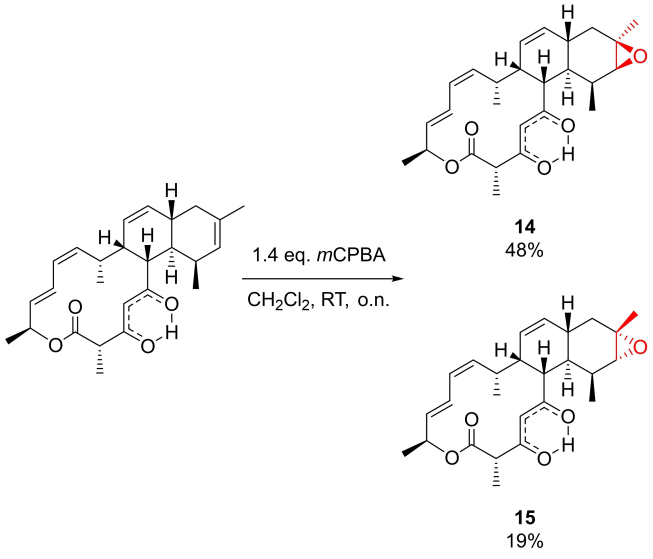

Scheme 4. Regioselective epoxidation of dehalogenil in the presence of *m*CPBA to the diastereomers **14** and **15**.

antimalarial activity of the class. In addition, compounds presenting an IC_{50} below 100 nM were also tested against mature transmission stages (stage IV–V gametocytes) of *P. falciparum*, resulting in low nanomolar activity (SI Table 4).

We aimed to identify key parts of the molecule and to further understand the role of different substituents regarding the SAR of the chlorotonil scaffold. Firstly, replacement of one carbonyl group to a bridged ether had a negative impact, resulting in complete loss of activity at tested concentrations when e.g. **2** is compared with the iodinated derivatives **SI6-8**. Interestingly, opening of the macrocycle resulted mostly in a drastic drop to complete loss of activity (**SI3-4** and **SI10-16**), but not systematically (**13** and **SI5**). Rearrangement of the macrocyle to **SI17** also led to complete loss of activity. It seems therefore that modifications can be brought to the macrocycle, but the diketone or vinylogous carboxylic acid moiety appears to be essential in this case.

Surprisingly and gratifyingly, complete dehalogenation still led to a highly active molecule. We observed excellent activity of **dehalogenil** against all Gram-positive bacteria in our test panel (MICs in sub-µg/mL range) and even higher activity (IC_{50} in single-digit nanomolar range) against *P. falciparum*. Interestingly, **14** still displayed a good activity

Table 1: Minimal inhibitory concentrations (MICs) against various Gram-positive bacterial strains and IC_{50} against *P. falciparum* of chlorotonil derivatives.

Compound	MIC [μg/mL][a]						IC_{50} [μM][b]	
	S. aureus	MRSA	*E. faecalis*	*E. faecium*	VRE	*S. epiderm.*	*P. falcip.* 3D7	*P. falcip.* Dd2
1	0.0125	0.05	0.025	0.0125	0.025	0.05	0.014 ± 0.005	0.016 ± 0.004
2	0.2	0.8	0.2	0.1	0.1	0.4	0.040 ± 0.004	0.045 ± 0.003
3	3.2	> 3.2	1.6	0.4	0.8	3.2	> 0.250	> 0.250
4	0.05	0.05	0.1	0.05	0.05	0.1	0.220 ± 0.029	0.372 ± 0.202
5	0.8	1.6	1.6	0.8	1.6	> 6.4	0.572 ± 0.021	0.415 ± 0.007
6	1.6	1.6	1.6	0.8	0.8	> 1.6	> 0.242	> 0.242
7	0.4	0.8	0.8	0.2	0.4	0.8	0.108 ± 0.003	0.071 ± 0.003
dehalogenil (8)	0.05	0.05	0.1	0.025	0.05	0.2	0.005 ± 0.002	0.0039 ± 0.0002
9	0.1	0.1	0.1	0.05	0.1	0.4	0.032 ± 0.001	0.066 ± 0.011
11	0.4	0.4	0.2	0.025	0.025	0.4	0.056 ± 0.002	0.065 ± 0.002
12	0.2	0.1	0.2	0.05	0.1	0.4	0.028 ± 0.000	0.060 ± 0.044
13	1.6	1.6	0.8	0.4	0.4	3.2	0.272 ± 0.019	0.573 ± 0.277
14	0.4	0.2	1.6	0.8	0.4	0.8	0.198 ± 0.016	0.142 ± 0.009
15	3.2	3.2	3.2	3.2	3.2	3.2	2.03 ± 0.182	2.05 ± 0.705
SI1	0.4	0.4	0.4	0.4	0.4	1.6	–	–
SI2	0.8	0.8	1.6	0.8	0.8	3.2	0.408 ± 0.173	0.385 ± 0.130
SI3	6.4	6.4	6.4	6.4	6.4	> 6.4	> 3.30	> 3.30
SI4	3.2	3.2	3.2	0.4	0.8	> 6.4	1.86 ± 0.037	2.47 ± 0.305
SI5	0.8	3.2	1.6	0.8	0.8	> 6.4	0.303 ± 0.053	0.329 ± 0.006
SI6	> 6.4	> 6.4	> 6.4	> 6.4	> 6.4	> 6.4	> 2.22	> 2.22
SI7	> 6.4	> 6.4	> 6.4	6.4	6.4	> 6.4	> 1.84	> 1.84
SI8	> 6.4	> 6.4	> 6.4	> 6.4	> 6.4	> 6.4	> 2.22	> 2.22
SI9	0.4	0.4	0.4	0.2	0.2	0.4	3.33 ± 1.75	1.89 ± 0.346
SI10	6.4	> 6.4	6.4	3.2	3.2	> 6.4	1.83 ± 0.203	1.86 ± 0.503
SI11	1.6	1.6	3.2	0.8	0.8	> 6.4	1.34 ± 0.623	1.61 ± 0.387
SI12	> 6.4	> 6.4	> 6.4	> 6.4	> 6.4	> 6.4	> 6.17	> 6.17
SI13	6.4	3.2	3.2	0.8	0.8	> 6.4	1.14 ± 0.141	1.19 ± 0.794
SI14	6.4	6.4	3.2	3.2	1.6	> 6.4	> 3.30	> 3.30
SI15	0.8	1.6	0.8	0.4	0.4	6.4	0.416 ± 0.049	0.791 ± 0.097
SI16	> 6.4	> 6.4	> 6.4	3.2	3.2	> 6.4	3.12 ± 0.260	> 3.30
SI17	> 6.4	> 6.4	> 6.4	> 6.4	> 6.4	> 6.4	> 3.02	> 3.02
Erythromycin	0.5	> 64	1	4	> 64	32	–	–
Clarithromycin	0.25	> 64	1	2	> 64	32	–	–

[a] MICs were determined using *S. aureus* Newman, *S. aureus* N315 (methicillin-resistant, MRSA), *Enterococcus faecalis* ATCC 29212, *Enterococcus faecium* DSM 20477, *Enterococcus faecium* DSM 17050 (vancomycin-resistant, VRE), *Staphylococcus epidermidis* DSM 28765. Starting concentration was set to 6.4 μg/mL, or adjusted based on activity range, and tested in twelve consecutive 2-fold dilutions. [b] Half-inhibitory concentrations (IC_{50}) are shown as mean ± SD ($n = 2$) and were determined for drug-sensitive *P. falciparum* 3D7 (chloroquine $IC_{50} = 7.4 \pm 2.6$ nM) and chloroquine-resistant *P. falciparum* Dd2 (chloroquine $IC_{50} = 226 \pm 76$ nM). **10** could not be tested due to limited compound availability. Compounds were dissolved in dimethyl suloxide (DMSO) and always added 1/900 to assay medium to achieve either the highest possible starting concentration or a starting concentration that supports calculating the IC_{50} reliably.

against *S. aureus*, albeit lower than **dehalogenil** (4 to 8-fold), but its activity dropped markedly against

Enterococcus spp. (16 to 32-fold). Moreover and analogously to **4** and its other epoxide isomer,[25] the stereochemistry of the epoxide has an influence on the activity as **15** is significantly less active than **14**. This finding strengthens the hypothesis that the conformation of this part of the compound is important.

When **SI1**, **8** and **12** were compared, the SAR revealed that the C2 methyl and its stereochemistry had an influence on the activity. Methyl substitution and *S*-configuration were most favorable. C4 functionalization had a substantial impact on antimicrobial activity with the substituent activity order of H/H > Cl/H > S_2H/H > F/Cl > Me/Cl when **8**, **2**, **11**, **5**, and **6** were compared. The trend of the activity of various substituents was even more pronounced in *P. falciparum* leading to more than 100-fold higher IC_{50} for **5** compared to **dehalogenil**. As shown earlier for epoxides,[20] C9 substitution with chlorine drastically lowered the activity against *P. falciparum* whereas the activity in bacteria was mostly retained. The obtained SAR findings are depicted in Figure 2. On top of the antibacterial and antimalarial activity profiling, we further performed a cytotoxicity screening of all derivatives against HepG2 cells. Remarkably, only **7** resulted in an IC_{50} of approximately 14 μg/mL, whereas all other derivatives were non-toxic up to the highest concentration tested (i.e. if possible 22.2 μg/mL unless otherwise noted, Supporting Information Table 5). Based on their antibacterial activity, the 27 new derivatives were categorized into three groups: nine were considered inactive (MIC ≥ 6.4 μg/mL), nine displayed moderate activity (MIC around 1 to 6.4 μg/mL), and nine retained activity (MIC below 1 μg/mL). Only derivatives with retained activity were considered and taken forward to further analyses, with the

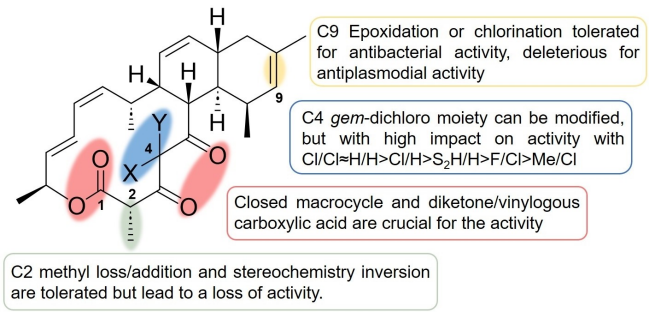

Figure 2. SAR overview of chlorotonils. Red: sites sensitive to change; green: modifiable sites; blue: dispensable sites.

exception of **15** that was also tested for structure-toxicity relationships studies. **SI9** was also excluded from group three despite showing good antibacterial activity as activity against *P. falciparum* dropped considerably.

The remaining derivatives with retained activity were subjected to toxicity profiling using zebrafish (*Danio rerio*) larvae (Table 2, Supporting Information Figure 3), a sensitive model useful to assess potential in vivo toxicity early on in a drug discovery campaign.[38,39] Derivatives were compared to the natural product **1** and the first-generation frontrunner **4** in a 48 h exposure setup starting three days post fertilization (dpf). All malformations and pathophysiological phenotypes were noted and used to determine the half-inhibitory concentration (IC_{50}) of the respective derivative against zebrafish larvae. The selectivity index (SI) (Table 2) was then calculated using MIC against *S. aureus* Newman and IC_{50} on *P. falciparum* 3D7 (as reported in Table 1). Overall, we sought to identify a molecule with retained activity in combination with favorable safety parameters even though there was no evidence from HepG2 testing and previous in vivo models that chlorotonils have a liability in safety. Generally, positions C2 and C4 seemed to be most important for selectivity, as Supporting Information dropped for **SI2** and **12**. Epoxidation at C9/10 significantly worsened selectivity as both **14** and **15** displayed toxicity in the one-digit micromolar range showing increased toxicity compared to **dehalogenil**. This could be related to the reactivity of the epoxide group. In order to assess the effect of the conformation, we tested both **14** and **15**.

Indeed, we observed that **14**, being significantly more active on *S. aureus*, also displays much higher toxicity on zebrafish larvae than its diastereoisomer **15** (1.22 vs. 9.85 μM, respectively). This confirms once more the importance of the 3D conformation at that side of the molecule. Nonetheless, both derivatives result in a similar selectivity index (Table 2). Overall, all new derivatives except **14** showed higher IC_{50} on larval development compared to **1** and **4**, respectively. It should be noted that e.g. **11** could have been also a potential candidate derivative with improved SI, however, compared to **dehalogenil** this derivative was approximately ten-fold less potent on the most important target pathogens *S. aureus* and *P. falciparum* and in addition, **11** could be only obtained as side product in low yield. Thus, **dehalogenil** seemed to be the most suitable molecule combining excellent in vitro activity with a much better Supporting Information for both *S. aureus* (SI = 225, compared to 41.7 and 10.5 for **1** and **4**, respectively) and *P. falciparum* (SI = 5480, compared to 77.8 and 5.2 for **1** and **4**, respectively). Together with its chemical accessibility, efficiency of purification and lack of potentially labile groups (no *gem*-dichloro moiety, no epoxide), we identified **dehalogenil** as the superior compound of this class; hence, we decided to further characterize **dehalogenil** aiming to assess its potential for nomination of a lead molecule.

Towards this end, we tested **dehalogenil** against multi-drug-resistant clinical isolates of *S. aureus* ($n = 100$ [MSSA/MRSA]; Table 3, Supporting Information Table 6) and *Enterococcus* spp. ($n = 98$ [VSE/VRE]; Table 4, Supporting Information Table 7). These tests confirmed excellent activity, notably with resistance-breaking properties. Drug resistance comprised erythromycin-resistance in 59 of the tested isolates, underlining that chlorotonils clearly represent a novel class of antibiotics and are not to be considered as conventional macrolide antibiotics. In contrast to the AWaRe reserve antibiotics and clinical standard of care competitors linezolid, daptomycin and tigecycline, **dehalogenil** MIC_{90}s were in an excellent sub-μg/mL range for both *S.*

Table 2: Half-inhibitory concentration (IC_{50}) of derivatives with retained activity tested against zebrafish larvae. Selectivity indices (SI) were calculated using *S. aureus* Newman and *P. falciparum* 3D7.

Derivative	IC_{50}[a] [μM]	Selectivity Index[b] *S. aureus*	*P. falciparum*
1	1.09	41.7	77.8
4	1.14	10.5	5.2
7	12.31	14.1	114.0
8 (Dehalogenil)	27.4	224.8	5479.6
9	8.25	39.9	257.7
11	>50	>62.5	>892.9
12	38.46	78.9	1373.7
14	1.22	1.30	6.2
15	9.85	1.31	4.9
SI1	33.24	35.8	–
SI2	27.03	13.4	66.2

[a] Half-inhibitory concentration was determined using zebrafish larvae in a 48 h exposure setup starting three days post fertilization on basis of pathophysiological phenotypes. [b] Selectivity index was calculated using the MIC or IC_{50} of the respective derivative as determined in Table 1.

Table 3: MIC distribution of **dehalogenil** and three clinically approved reserve antibiotics in clinical isolates of *S. aureus* ($n = 100$; MSSA and MRSA).

Compound	MIC range [μg/mL]	MIC_{50} [μg/mL][a]	MIC_{90} [μg/mL][b]
dehalogenil	0.025–0.4	0.1	0.2
linezolid	2–>64	4	8
daptomycin	0.25–>64	0.5	4
tigecycline	1–16	4	8

[a] Concentration inhibiting growth in ≥50% of all tested isolates. [b] Concentration inhibiting growth in ≥90% of all tested isolates. For more details, see Supporting Information Table 6.

Table 4: MIC distribution of **dehalogenil** and three clinically approved reserve antibiotics in clinical isolates of *E. faecalis* and *E. faecium* ($n=98$).

Compound	MIC range [μg/mL]	MIC_{50} [μg/mL][a]	MIC_{90} [μg/mL][b]
dehalogenil	0.00625–0.2	0.025	0.1
linezolid	0.5–64	4	4
daptomycin	0.5–4	2	4
tigecyclin	0.5–16	2	2

[a] Concentration inhibiting growth in ≥50% of all tested isolates. [b] Concentration inhibiting growth in ≥90% of all tested isolates. For more details, see Supporting Information Table 7.

aureus and *Enterococcus* spp. With unimodal MIC distribution indicating no pre-existing resistance in these clinical strain collections.

Next, we determined absorption, distribution, metabolism, and excretion (ADME) properties of **dehalogenil**. This has only been partly possible for the first-generation frontrunner **4** or the natural product **1** because of their poor limit of detection in LCMS-based methods and insufficient solubility. Overall, **dehalogenil** showed a favorable ADME profile (Table 5). The solubility more than doubled at physiological pH 7.4 when compared to **4** (kinetic solubility, 16.2±4.9 μM) and increased more than 500-fold compared to the natural product **1**.[25] Therefore, **dehalogenil** has the best water solubility compared to **1** and **4** and favorable (reduced) lipophilicity as suggested by cLogP (SI Table 8).

Across species (mouse, rat, human), metabolic stability of **dehalogenil** was high while plasma stability was moderate. Besides, no hemolysis and no significant inhibition of the metabolically important enzyme CYP3 A4 was observed. However, plasma protein binding (PPB) was >99.4% in all species. This finding was expected considering the poor water solubility of the compound class and is in line with an observed drop in in vitro activity in the presence of fetal bovine serum (FBS). Already at 5% FBS, **4** showed an over 100-fold shift as opposed to 32-fold for both **1** and **dehalogenil** (SI Table 9). Importantly, under standard conditions for such assessments, i.e. supplementing with 6% bovine serum albumin (BSA), we observed only 4-fold reduced antimicrobial activity of **1** and **dehalogenil**, respectively, whereas the antimicrobial activity of **4** dropped already by 32-fold, further underlining the superiority of the second-generation frontrunner. Despite the relatively low amount of free drug to be expected in vivo, we were encouraged by these overall findings, considering the remarkable potency of the compound class. Furthermore, we have previously demonstrated in vivo efficacy of **4**[25] and, hence, expected **dehalogenil** to show even better results in vivo.

In a first step, we determined blood levels of **dehalogenil** administered perorally in soy oil in a pharmacokinetic (PK) study in mice (Figure 3 and Table 6) analogously to a previous study with **4**.[25] Here, we found significantly higher blood levels for **dehalogenil** compared to **4** as characterized by an about 4-fold higher C_{max} and about 5- to 6-fold higher $AUC_{0\text{-}tz}$ of **dehalogenil** compared to **4**. Clearance was slow ($t_{1/2z}$ of 5.5 and 10 h for 10 and 50 mg/kg, respectively) but considerably faster than for **4**.

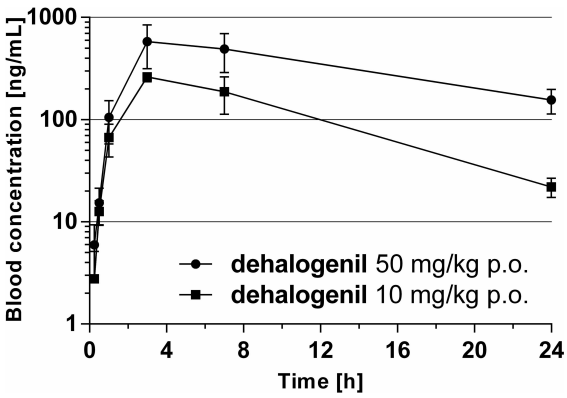

Figure 3. Pharmacokinetics in mice ($n=3$) after p.o. administration of 10 or 50 mg/kg dehalogenil in soy oil. Mean and SD are shown.

Table 5: Physicochemical and ADME parameters of **dehalogenil**.

Semi thermodynamic solubility [μM][a]	pH 5.0 34.9±2.7	pH 7.4 41.4±10.3	pH 9.0 16.5±8.7
	mouse	rat	human
Microsomal clearance [μL/min/mg protein][b]	6.4	14	6.4
Plasma stability $t_{1/2}$ [h]	1.5	1.2	1.4
Plasma protein binding [%][c]	>99.8	>99.4	>99.6
CYP3 A4 inhibition[d]	16.4 μM		
Hemolysis of human blood cells @ 20 μM[e]	1.40%		

[a] Kinetic solubility at pH 7 for **1**: 0.073±0.005 μM and **4**: 16.2±4.9 μM.[25] [b] 1 μM test compound in 0.5% DMSO. As reference, we obtained microsomal clearance of 221—363 μL/min/mg protein for verapamil. [c] 10 μM test compound in 0.5% DMSO was used. As reference, we observed plasma protein binding of 93.8%, 99.1% or 99.5% at pH 5.0, pH 7.4 or pH 9.0 respectively by warfarin. [d] As reference, we observed CYP3A4 inhibition with an IC_{50} of 0.021 μM by ketoconazole. [e] Baseline of hemolysis is at 1.4%.

Table 6: PK parameters given as mean ($n=3$) of **dehalogenil** and **4** in mice after p.o. administration in soy oil.

Parameters[a]	Dehalogenil 10 mg/kg, p.o.[b]	Dehalogenil 50 mg/kg, p.o.[b]	4[c] 10 mg/kg, p.o.[b]	4[c] 50 mg/kg, p.o.[b]
C_{max} [ng/mL]	261	579	75.3	147.7
t_{max} [h]	3	3	3	3
t_z [h]	24	24	18	24
$t_{1/2z}$ [h]	5.5	10.2	31.9	n.c.
$AUC_{0\text{-}tz}$ [ng*h/mL]	3022	8359	603	1409

[a] C_{max}: maximum concentration; t_{max}: time at which C_{max} is reached; t_z: time of the last sample, which has an analytical quantifiable concentration; $t_{1/2z}$: half-life of the terminal slope of a concentration-time curve between t_0 and t_z; $AUC_{0\text{-}tz}$: area under the concentration-time curve up to the time t_z. [b] compounds were given orally in soy oil formulation. [c] **4** blood PK was taken from Hofer et al.[25] and displayed again for head-to-head comparison.

To identify a vehicle suitable for i.v. administration, we attempted different formulations including commercially available ClearSol™ CSV-2 (Latitude). This formulation dissolved **dehalogenil** in concentrations of >10 mg/mL and can be used after 1:1 dilution (*v/v*) with e.g. saline. Hence, we were for the first time able to determine blood PK after i.v. administration for this compound class (Figure 4, Table 7). Based on this, the oral bioavailability of **dehalogenil** dissolved in soy oil was determined to be 9.5 %.

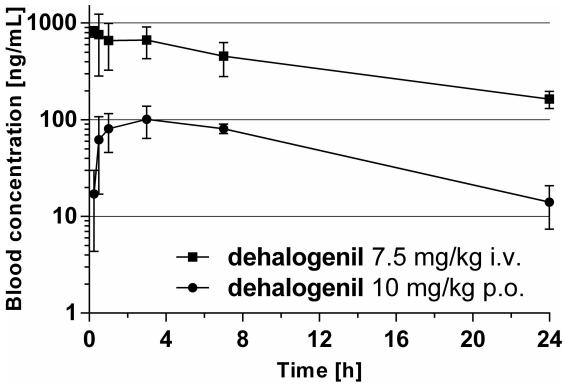

Figure 4. Pharmacokinetics in mice ($n=3$) after i.v and oral administration of 7.5 or 10 mg/kg **dehalogenil** in soy oil or CSV-2/saline respectively. Mean and SD are shown.

Table 7: Selected PK parameters given as mean ($n=3$) of **dehalogenil** in mice after i.v. (CSV-2/saline) or oral administration (soy oil).

Dehalogenil Parameters[a]	10 mg/kg p.o.[b]	7.5 mg/kg i.v.[c]
C_0 [ng/mL]	–	872
C_{max} [ng/mL]	101	–
t_{max} [h]	3	–
t_z [h]	24	24
$t_{1/2z}$ [h]	6.7	10.8
$AUC_{0\text{-}tz}$ [ng*h/mL]	1400	9575
AUC (0-inf) [ng*h/mL]	1537	12120
Bioavailability [%]	9.5	100

[a] C_0: concentration at time zero; C_{max}: maximum concentration; t_{max}: time at which c_{max} is reached; t_z: time of the last sample, which has an analytically quantifiable concentration; $t_{1/2z}$: half-life of the terminal slope of a concentration-time curve between t_0 and t_z; $AUC_{0\text{-}tz}$: area under the concentration-time curve up to the time t_z; $AUC_{0\text{-}inf}$: area under the concentration-time curve extrapolated to infinity. **Dehalogenil** was given p.o [b] or intravenously [c] in CSV-2/saline.

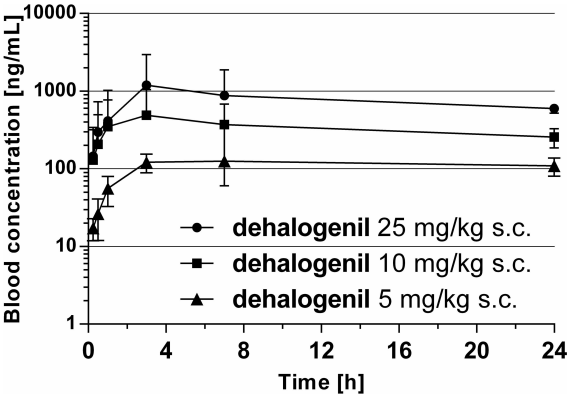

Figure 5. Pharmacokinetics in mice ($n=3$) after subcutaneous application of 5, 10 or 25 mg/kg **dehalogenil** in CSV-2/saline. Mean and SD are shown.

In preparation of in vivo efficacy studies, we sought to check additional application routes including subcutaneous (s.c.) injection using **dehalogenil** again dissolved in CSV-2/saline (Figure 5 and Table 8). **Dehalogenil** was applied at 5, 10 and 25 mg/kg and both blood levels and AUC were found to be dose-proportional. Compared to p.o. and i.v. routes, the s.c. administration of **dehalogenil** was mainly characterized by a significantly longer half-time, and a single daily dose of 25 mg/kg appeared to be suitable for mouse infection models since blood levels stayed above the MIC for ≥24 h. For this reason, we preferred s.c. dosing for the pharmacodynamics studies in order to obtain in vivo proof-of-concept for infections caused by *S. aureus.*

First, we decided to evaluate the in vivo activity of **dehalogenil** using a murine foreign body infection model.[37] Here, 1 cm peripheral venous catheter fragments were implanted subcutaneously into the flanks of mice, infected with 10^4 CFU of the biofilm-forming *S. aureus* strain SA113, and then treated s.c. using **dehalogenil** dissolved in CSV-2. Treatment with a dose of 25 mg/kg body weight of **dehalogenil** once per day for a period of six days resulted in a significant reduction of the bacterial load on the catheter fragment and in the tissue surrounding the catheter fragment when compared to the sham-treated controls, which received CSV-2 only (Figures 6a and b).

Importantly, s.c. treatment with **dehalogenil** led to >3-log_{10} reduction in bacterial loads found on the catheter fragments (3.85-log_{10}) and the tissues (3.24-log_{10}) surrounding the catheter fragments, respectively, suggesting a high antibacterial activity of **dehalogenil** against *S. aureus* in this in vivo infection model. Notably, CFU rates recovered from catheter fragments and tissue of **dehalogenil**-treated mice were even more than 1-log_{10} smaller than those seen in mice treated with 25 mg/kg of the reserve antibiotic linezolid once per day (Figure 6a and b).

Table 8: PK parameters ($n=3$) of **dehalogenil** in mice after subcutaneous application in CSV-2/saline.

Dehalogenil Parameters[a]	5 mg/kg s.c.[b]	10 mg/kg s.c.[b]	25 mg/kg s.c[b]
C_{max} [ng/mL]	125.0	488.0	1195
t_{max} [h]	7.0	3.0	3.0
t_z [h]	24.0	24.0	24.0
$t_{1/2z}$ [h]	NC	NC	NC
$AUC_{0\text{-}tz}$ [ng*h/mL]	2689	8090	18548

[a] C_{max}: maximum concentration; t_{max}: time at which C_{max} is reached; t_z: time of the last sample, which has an analytically quantifiable concentration; $t_{1/2z}$: half-life of the terminal slope of a concentration-time curve between t_0 and t_z; $AUC_{0\text{-}tz}$: area under the concentration-time curve up to the time t_z.; NC: non-calculable [b] **dehalogenil** was given subcutaneously in CSV-2/saline.

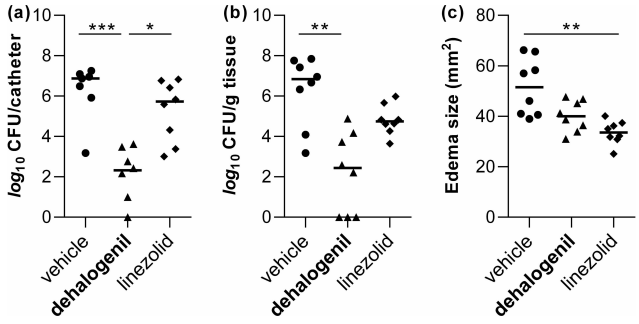

Figure 6. In vivo efficacy of **dehalogenil** in an *S. aureus* related murine foreign body infection model. The infection was established using a bacterial inoculum of 1×10^4 colony-forming units (CFU) injected into the lumen of the implanted peripheral venous catheter tubing fragment. **Dehalogenil** (25 mg/kg) was administered s.c. once per day, starting at 3 h post infection. Linezolid (Zyvoxid, Pfizer; 25 mg/kg s.c.) was used as a reference antibiotic. Six days post infection, mice were euthanized, edema sizes around the implanted catheter fragments determined (c), and the catheter fragments and surrounding tissues were explanted. Bacterial loads from catheter detached biofilms (a) and in surrounding tissue homogenates (b) were determined by CFU counting. The data represent the value of every individual animal (symbols) and the median (horizontal lines). $*p<0.05$, $**p<0.01$, $***p<0.001$ (Kruskal-Wallis tests followed by Dunn's post hoc test).

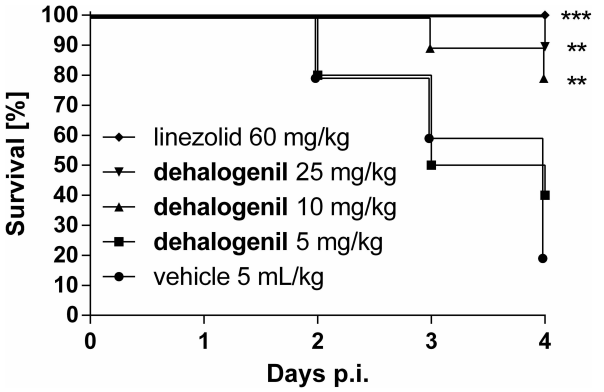

Figure 7. Survival rates in a sepsis model with **dehalogenil**, vehicle and linezolid (60 mg/kg) given subcutaneously in CD-1 mice ($n=10$). Mice were infected intravenously using *S. aureus* USA300LAC (10^8 CFU/mice). Compounds were administered twice daily starting 4 hours post infection (p.i.) until day 3 p.i., with the daily total dose indicated. Curves were compared via Mantel-Cox test (Prism), with ***: $p<0.001$ and **: $p<0.01$.

This effect was particularly evident for the CFU numbers recovered from the catheter tubing of *S. aureus* SA113 infected mice treated with **dehalogenil**, which were in the mean more than 3-log_{10} smaller than those recovered from infected mice treated with linezolid (Figure 6a). However, when edema sizes were compared at day six post infection (p.i.), only linezolid treatment allowed for a significant reduction in edema size formation at the infection site, while this reduction was not significant for **dehalogenil** (Figure 6c).

Taken together, these findings suggest that **dehalogenil** is superior over linezolid in both reducing the bacterial population formed by *S. aureus* on an implanted medical device, and to suppress the dissemination of the bacteria into the surrounding tissue. Linezolid, on the other hand, seems to be more effective than **dehalogenil** in suppressing the expansion of the inflammation at the infection site. In none of the infected mice, any bacteria were found in blood samples collected at six days p.i., demonstrating that none of the catheter tubing infected mice became systemically infected during the experiment.

Next, we moved to a more severe and challenging model and decided to test **dehalogenil** in a *Staphylococcus* blood infection (sepsis) model, alongside linezolid as reference compound (Figure 7). Mice were infected using *S. aureus* strain USA300LAC (10^8 CFU/animal) and subsequently treated with a daily total dose of 5, 10 or 25 mg/kg **dehalogenil**, split into two doses (8 h interval, BID regimen, s.c), until 3 days p.i.. Remarkably, treatment with 10 and 25 mg/kg **dehalogenil** resulted in significantly improved survival rates (80 % and 90 %, respectively) compared to 20 % in the untreated control group, while 60 mg/kg linezolid resulted in the survival of all animals.

Thus, we have demonstrated here that **dehalogenil** is able to rescue severely infected mice underlining the potential of this promising class of natural compounds. Optimization through semisynthetic modification was key to this success. Taken together with the potent in vitro activity, improved physicochemical properties and favorable safety of the molecule, we therefore consider **dehalogenil** as a lead compound for the development as a novel anti-infective with resistance-breaking properties.

Conclusion

Although chlorotonils show poor reactivity, we could successfully demonstrate new ways of obtaining semisynthetic derivatives with modifications targeting various positions of the carbon backbone. Some compounds were obtained in small amounts as fermentation side products. Besides, we did not only observe new regio- and stereoselective reactions but also discovered a new sulfur-mediated dehalogenation reaction. Different chemical moieties influencing activity against multidrug-resistant Gram-positive bacteria and *P. falciparum* were assessed, revealing the positions C2 and C4 as particularly important for activity.

These studies revealed the second-generation frontrunner **dehalogenil** as the novel lead compound.[40] In contrast to previous frontrunner **4**, **dehalogenil** retained superb antimicrobial activity not only against Gram-positive bacteria but also against *Plasmodium*, while further showing significantly improved water solubility and selectivity. Unlike previous reports on dehalogenated chlorotonil A[23,41] being biologically inactive, we present here an alternative semisynthetic route to this derivative. We could clearly validate its structure through NMR studies and confirmed its biological activity. Furthermore, we did not determine a particular critical ADMET parameter, but PPB is an

obvious optimization goal to increase the free fraction and further improve in vivo activity. **Dehalogenil** could be administered orally up to 50 mg/kg with increased blood concentrations compared to **4** and an oral bioavailability of around 10 % in a non-optimized formulation. We consider this a promising starting point for the optimization of peroral bioavailability, e.g. via formulation development or a pro-drug approach. We have demonstrated excellent in vivo activity in *S. aureus* infected mice after s.c. administration of **dehalogenil** in both a local infection model and a severe systemic infection model. These results led us to nominate **dehalogenil** as a lead compound with potential for clinical application as novel resistance-breaking anti-infective agent.

Acknowledgements

We want to thank Axel Schulz, Christin Löhner, Max Niehage, Andrew Perreth and Reinhard Sterlinski for the help with the large-scale fermentation of chlorotonils. We thank Kerstin Schober and Rolf Jansen for the help with downstream processing after fermentation. Instrumentation and technical assistance for this work were provided by the Service Center X-ray Diffraction, with financial support from Saarland University and German Science Foundation (project number INST 256/506-1). The project was funded by the German Federal Ministry of Education and Research as part of the ChloroClinaria grant provided to Rolf Müller (16GW0204K), Jana Held (16GW0206) and Markus Bischoff (16GW0230) as well as Helmholtz Pre-4D funding. Open Access funding enabled and organized by Projekt DEAL.

Conflict of Interest

The authors declare no conflict of interest.

Data Availability Statement

The data that support the findings of this study are available in the supplementary material of this article.

Keywords: anti-infectives · chlorotonil · natural products · pharmacokinetics · zebrafish

[1] A. G. Atanasov, S. B. Zotchev, V. M. Dirsch, I. E. Orhan, M. Banach, J. M. Rollinger, D. Barreca, W. Weckwerth, R. Bauer, E. A. Bayer, M. Majeed, A. Bishayee, V. Bochkov, G. K. Bonn, N. Braidy, F. Bucar, A. Cifuentes, G. D'Onofrio, M. Bodkin, M. Diederich, A. T. Dinkova-Kostova, T. Efferth, K. El Bairi, N. Arkells, T.-P. Fan, B. L. Fiebich, M. Freissmuth, M. I. Georgiev, S. Gibbons, K. M. Godfrey, C. W. Gruber, J. Heer, L. A. Huber, E. Ibanez, A. Kijjoa, A. K. Kiss, A. Lu, F. A. Macias, M. J. S. Miller, A. Mocan, R. Müller, F. Nicoletti, G. Perry, V. Pittalà, L. Rastrelli, M. Ristow, G. L. Russo, A. S. Silva, D. Schuster, H. Sheridan, K. Skalicka-Woźniak, L. Skaltsounis, E. Sobarzo-Sánchez, D. S. Bredt, H. Stuppner, A. Sureda, N. T. Tzvetkov, R. A. Vacca, B. B. Aggarwal, M. Battino, F. Giampieri, M. Wink, J.-L Wolfender, J. Xiao, A. W. K. Yeung, G. Lizard, M. A. Popp, M. Heinrich, I. Berindan-Neagoe, M. Stadler, M. Daglia, R. Verpoorte, C. T. Supuran, *Nat. Rev. Drug Discovery* **2020**, *131*, 65–71.
[2] G. D. Wright, *Nat. Prod. Rep.* **2017**, *34(7)*, 694–701.
[3] D. Camp, R. A. Davis, M. Campitelli, J. Ebdon, R. J. Quinn, *J. Nat. Prod.* **2012**, *75*, 72–81.
[4] D. J. Newman, G. M. Cragg, *J. Nat. Prod.* **2020**, *83*, 770–803.
[5] A. Kerschning, F. Hahn, *Angew. Chem. Int. Ed.* **2012**, *51*, 4012–4022.
[6] N. Skrzypczaka, P. Przybylski, *Nat. Prod. Rep.* **2022**, *39*, 1678–1704.
[7] D. J. Vollmann, L. Winand, M. Nett, *Curr. Opin. Biotechnol.* **2022**, *77*, 102761.
[8] C. I. Ventola, *P. T.* **2015**, *40*, 277–283.
[9] H. W. Boucher, *Trans. Am. Clin. Climatol. Assoc.* **2020**, *131*, 65–71.
[10] S. Baron, L. Hadjadj, J.-M. Rolain, A. O. Olaitan, *Int. J. Antimicrob. Agents* **2016**, *48(6)*, 583–591.
[11] K. J. Wicht, S. Mok, D. A. Fidock, *Annu. Rev. Microbiol.* **2020**, *74*, 431–454.
[12] L. E. Buyon, B. Elsworth, M. T. Duraisingh, *Int. J. Parasitol. Drugs Drug Resist.* **2021**, *16*, 23–37.
[13] M. A. Fischbach, C. T. Walsh, *Science* **2009**, *325*, 1089–1093.
[14] J. N. Burrows, S. Duparc, W. E. Gutteridge, R. H. van Huijsduijnen, W. Kaszubska, F. Macintyre, S. Mazzuri, J. J. Möhrle, T. N. C. Wells, *Malar. J.* **2017**, *16(26)*.
[15] C. T. Walsh, T. A. Wencewicz, *J. Antibiot. Res.* **2014**, *67*, 7–22.
[16] M. Miethke, M. Pieroni, T. Weber, M. Brönstrup, P. Hartmann, L. Halby, P. B. Arimondo, P. Glaser, B. Aigle, H. B. Bode, R- Moreira, Y. Li, A. Luzhetskyy, M. H. Medema, J.-L. Pernodet, M. Stadler, J. T. Tormo, O. Genillaud, A. W. Truman, K. J. Weissman, E. Takano, S. Sabatini, E. Stegmann, H. Brötz-Oesterhelt, W. Wohlleben, M. Seemann, M. Empting, A. K. H. Hirsch, B. Loretz, C.-M. Lehr, A. Titz, J. Herrmann, T. Jaeger, S. Alt, T. Hesterkamp, M. Winterhalter, A. Schiefer, K. Pfarr, A. Hoerauf, H. Graz, M. Graz, M. Lindvall, S. Ramurthy, A. Karlén, M. van Dongen, H. Petkovic, A. Keller, F. Peyrane, S. Donadio, L. J. V. Piddock, I. H. Gilbert, H. E. Moser, R. Müller, *Nat. Chem. Rev.* **2021**, *5*, 726–749.
[17] O. Genilloud, *Curr. Opin. Microbiol.* **2019**, *51*, 81–87.
[18] G. D. Wright, *Nat. Prod. Rep.* **2017**, *34(7)*, 694–701.
[19] K. Gerth, H. Steinmetz, G. Höfle, R. Jansen, *Angew. Chem. Int. Ed.* **2008**, *47*, 600–602.
[20] S. Walesch, J. Birkelbach, G. Jézéquel, F. P. J. Haeckl, J. D. Hegemann, T. Hesterkamp, A. K. H. Hirsch, P. Hammann, R. Müller, *EMBO Rep.* **2023**, *24*, e56033.
[21] A. Janas, P. Przybylski, *Eur. J. Med. Chem.* **2019**, *182*, 111662.
[22] A. Janas, K. Pyta, M. Gdaniec, P. Przybylski, *J. Org. Chem.* **2022**, *87*, 3758–3761.
[23] J. Held, T. Gebru, M. Kalesse, R. Jansen, K. Gerth, R. Müller, B. Mordmüller, *Antimicrob. Agents Chemother.* **2014**, *58*, 6378–6384.
[24] K. Jungmann, R. Jansen, K. Gerth, V. Huch, D. Krug, W. Fenical, R. Müller, *ACS Chem. Biol.* **2015**, *10*, 2480–2490.
[25] W. Hofer, E. Oueis, A. A. Fayad, F. Deschner, A. Andreas, L. P. de Carvalho, S. Hüttel, S. Bernecker, L. Pätzold, B. Morgenstern, N. Zaburannyi, M. Bischoff, M. Stadler, J. Held, J. Herrmann, R. Müller, *Angew. Chem. Int. Ed.* **2022**, e202202816.
[26] H. Finkelstein, *Ber. Dtsch. Chem. Ges.* **1910**, *43*, 1528–1532.
[27] T. Sala, M. V. Sargent, *J. C. S. Chem. Comm.* **1978**, 253–254.
[28] N. Rahn, M. Kalesse, *Angew. Chem. Int. Ed.* **2008**, *47*, 597–599.
[29] T. Chivers, P. J. W. Elder, *Chem. Soc. Rev.* **2013**, *42*, 5996–6005.

[30] Z.-Y. Gu, J.-J. Cao, S.-Y. Wang, S.-J. Ji, *Chem. Sci.* **2016**, *7*, 4067–4072.
[31] G. Zhang, H. Yi, H. Chen, C. Bian, C. Liu, A. Lei, *Org. Lett.* **2014**, *16*, 6156–6159.
[32] F. Su, S. Chen, X. Mo, K. Wu, J. Wu, W. Lin, Z. Lin, J. Lin, H.-J. Zhang, T.-B. Wen, *Chem. Sci.* **2020**, *11*, 1503–1509.
[33] M. Wang, Q. Fan, X. Jiang, *Org. Lett.* **2016**, *18*, 5756–5759.
[34] J. L. Jat, M. P. Paudyal, H. Gao, Q.-L. Xu, M. Yousufuddin, D. Devarajan, D. H. Ess, L. Kürti, J. R. Falck, *Science* **2014**, *343*, 61–65.
[35] F. Bendrath, V. Specowius, D. Michalik, P. Langer, *Tetrahedron* **2012**, *68*, 6456–6462.
[36] Z. Ma, Z. Zhou, L. Kürti, *Angew. Chem. Int. Ed.* **2017**, *56*, 9886–9890.
[37] L. Pätzold, A.-C. Brausch, E.-L. Bielefeld, L. Zimmer, G. A. Somerville, M. Bischoff, R. Gaupp, *Microorganisms* **2021**, *9(3)*, 466.
[38] E. E. Patton, L. I. Zon, D. M. Langenau, *Nat. Rev. Drug Discovery* **2021**, *20*, 611–628.
[39] I. Miyawaki, *J. Toxicol. Pathol.* **2020**, *33(4)*, 197–210.
[40] Patent application EP23172607.6 **2023**.
[41] N. Rahn, *Die Totalsynthese von Chlorotonil A. Dissertation.* Gottfried Wilhelm Leibniz University Hanover **2007**.

Manuscript received: December 21, 2023
Accepted manuscript online: March 19, 2024
Version of record online: April 3, 2024